

**Towards a better understanding of the origins of microlens arrays in Mesozoic ophiuroids
and asteroids**

Przemysław Gorzelak^{1*}, Imran A. Rahman², Samuel Zamora^{3,4}, Arkadiusz Gąsiński⁵, Jerzy
Trzciński⁶, Tomasz Brachaniec⁷, and Mariusz A. Salamon^{8*}

¹Institute of Paleobiology, Polish Academy of Sciences, Twarda 51/55, 00-818 Warsaw, Poland,
email: pgorzelak@twarda.pan.pl

²Oxford University Museum of Natural History, Parks Road, Oxford, OX1 3PW, United
Kingdom

³Instituto Geológico y Minero de España (IGME), C/Manuel Lasala, 44, 9ºB, 50006, Zaragoza,
Spain

⁴Unidad Asociada en Ciencias de la Tierra, Universidad de Zaragoza-IGME, Zaragoza, Spain

⁵Institute of Geochemistry, Mineralogy and Petrology, Faculty of Geology, University of
Warsaw, Żwirki i Wigury 93, 02-089 Warsaw, Poland

⁶Institute of Hydrogeology and Engineering Geology, Faculty of Geology, University of
Warsaw, Żwirki i Wigury 93, 02-089 Warsaw, Poland

⁷Department of Geochemistry, Mineralogy and Petrography, Faculty of Earth Sciences,
University of Silesia, Będzińska 60, 41-200 Sosnowiec, Poland

⁸Department of Palaeontology and Stratigraphy, Faculty of Earth Sciences, University of Silesia,
Będzińska 60, 41-200 Sosnowiec, Poland.

Abstract

Echinoderms are characterized by a calcite endoskeleton with a unique microstructure, which is optimized for multiple functions. For instance, some light-sensitive ophiuroids (Ophiuroidea) and asteroids (Asteroidea) possess skeletal plates with multi-lens arrays that are thought to act as photosensory organs. The origins of these lens-like microstructures have long been unclear. It was recently proposed that the complex photosensory systems in certain modern ophiuroids and asteroids could be traced back to at least the Late Cretaceous (ca. 79 Ma). Here, we document similar structures in ophiuroids and asteroids from the Early Cretaceous of Poland (ca. 136 Ma) that are approximately 57 million years older than the oldest asterozoans with lens-like microstructures described thus far. We use scanning electron microscopy, synchrotron tomography, and electron backscatter diffraction combined with focused ion beam microscopy to describe the morphology and crystallography of these structures in exceptional detail. The results indicate that, similar to Recent light-sensitive ophiuroids, putative microlenses in Cretaceous ophiuroids and asteroids exhibit a shape and crystal orientation that would have minimized spherical aberration and birefringence. We suggest that these lens-like microstructures evolved by secondary deposition of calcite on pre-existing porous tubercles that were already present in ancestral Jurassic forms.

Key words: echinoderms, photosensitivity, Cretaceous, microlenses, calcite, tomography

Introduction

Echinoderms exploit their calcite endoskeleton for a variety of functions, including support, movement, protection, food gathering, and ion storage (Smith 1990). This multipurpose tissue

47 can be modelled into different shapes through the use of an amorphous calcium carbonate
48 precursor and the involvement of organic molecules during the biomineralization process (e.g.
49 Politi et al. 2004; Killian and Wilt 2008). The role of the echinoderm skeleton in vision was
50 suggested long ago (Raup 1966), but it is only recently that scientists have begun to examine this
51 phenomenon more closely. For instance, it has been shown that some sea urchins use their
52 skeleton as a shielding device for photoreceptor cells, forming numerous compound eye units
53 (Ullrich-Lüter et al. 2011). Another, strikingly different example of using the skeleton as a part
54 of the photoreceptive system is reported for the light-sensitive ophiocomid ophiuroid *Ophiocoma*
55 *wendtii* (Hendler and Byrne 1987). This species changes colour from uniformly dark brown
56 during the day to grey and black banded at night when it is most active (Hendler 1984). This
57 change is not connected with camouflage, but is related to their sensitivity to light (Hendler
58 2004). Indeed, it has been shown that this species possesses calcitic microlens arrays, surrounded
59 by pigment-filled chromatophores, which are able to focus light onto presumably light-sensitive
60 nerve bundles (Aizenberg et al. 2001). These microlenses are micron-scale in size, lightweight,
61 mechanically strong, aberration-free, and birefringence-free, all properties that may be applicable
62 to materials science (Zhang 2003; Aizenberg and Hendler 2004). Such lens-like microstructures
63 are also present in other light-sensitive ophiocomid species, but do not occur in light-insensitive
64 species (Hendler and Byrne 1987). Interestingly, photosensitive proteins (both rhabdomeric and
65 ciliary opsins) have been recently identified in the arms of the ophiocomid *Ophiopsila aranea*,
66 which possesses similar lens-like microstructures (Delroisse et al. 2016). This species exhibits a
67 high sensitivity to green wavelengths of light, indicating a directional phototaxis likely enhanced
68 by the microlenses (Delroisse et al. 2016).

Comparable, though not homologous, structures are also present in some shallow-water asteroids (e.g. goniasterids and archasterids) that live within the photic zone (e.g. Mah 2005; Vinogradova et al. 2016). Although focusing light through microlens arrays has yet to be confirmed in these taxa, their morphology is strikingly similar to the microlenses of ophiocomid ophiuroids, and they are thus considered to be involved in photoreception (e.g. Döderlein 1898; Hendler and Byrne 1987; Dubois and Hayt 1990; Mah 2005; Vinogradova et al. 2016). Notably, in the case of the asteroid *Iconaster*, it has recently been shown that the microlenses are largely absent in deep-water sister and outgroup taxa, implying that their convergent expression is related to the exposure to sunlight (Mah 2005). The origin of microlens arrays in asterozoans (the clade comprising ophiuroids and asteroids) is unclear. Similar lens-like microstructures were recently documented in some Late Cretaceous ophiuroids and asteroids from Poland, implying that the origins of these putative complex photosensory systems should be traced back to at least the Campanian (ca. 79 Ma) (Gorzelak et al. 2014). Although external faces in fossil asterozoans are commonly covered by various types of granular ornamentation, sometimes referred to as tubercles or pustules (e.g. Blake et al. 2000; Villier et al. 2004), in-depth microstructural investigations and functional interpretations of these structures are largely lacking. In this paper, we use state-of-the-art imaging techniques to describe the morphology of isolated plates from the arms of select Mesozoic ophiuroids and asteroids, and compare these to modern specimens with lens-like microstructures. The results shed light on the origins and development of microlens arrays in asterozoans.

Materials and Methods

Isolated asterozoan plates with lens-like microstructures were collected by one of us (MAS) during the course of field work on Cretaceous crinoids (Salamon 2009). The material came from late Valanginian (ca. 136 Ma) silts intercalated with clayey sands, which are exposed in an abandoned brick-pit in Wąwał near Tomaszów Mazowiecki (central Poland, 51°29'50''N 20°3'05''E, see Kaim 2001). For comparative purposes, we also surveyed mostly isolated plates (>2000 elements in total) of shallow-water ophiuroids and asteroids (mainly belonging to the families Ophiuridae, Goniasteridae, Astropectinidae and Benthoplectinidae) from the Triassic, Jurassic and Cretaceous of Poland, Lithuania and Czech Rep., which are housed in the collections of the Department of Earth Sciences, Laboratory of Palaeontology and Biostratigraphy, University of Silesia (GIUS), Sosnowiec, Poland (Electronic Supplementary Material; for detailed description of sampling sites see Salamon and Zatoń 2007; Salamon 2008; Villier 2008; Zatoń et al. 2008; Gorzelak and Salamon 2009; Salamon and Gorzelak 2010; Hess et al. 2011; Salamon et al. 2012).

Plates of a specimen of the Recent photosensitive ophiuroid *O. wendtii* from southeastern Florida, which displays lens-like microstructures, were also investigated. Soft tissues in this ophiuroid were removed by soaking the specimen in a 5% sodium hypochlorite solution for 2 hours at room temperature.

High-resolution observations on carbon-coated plates of Recent and fossil specimens were performed with a Philips XL-20 Scanning Electron Microscope (SEM) at the Institute of Paleobiology of the Polish Academy of Sciences in Warsaw (accelerating voltage = 25 kV, working distance = 34 mm). In addition, the three-dimensional microstructure of select plates was studied using non-destructive propagation-based phase-contrast synchrotron radiation X-ray tomographic microscopy. The small size of the samples and their low attenuation contrast

necessitated high-resolution synchrotron-based phase-contrast imaging instead of conventional lab-based X-ray micro-tomography (Sutton et al. 2014; Cunningham et al. 2014). Tomography was performed at the TOMCAT beamline (Stampanoni et al. 2007) of the Swiss Light Source, Paul Scherrer Institut, Villigen, Switzerland. The specimens was mounted on SEM stubs with nail polish and scanned at 4× optical magnification using an X-ray energy of 20 keV, 1501 projections, and an exposure time of 125 ms. The detector consisted of a 20-μm thick LAG:Ce scintillator and a CCD camera, and the distance between the sample and the detector (propagation distance) was set at 40 mm. Slices were reconstructed using in-house software, including custom algorithms for ring artefact reduction and phase retrieval. This provided tomographic datasets with a voxel size of 1.625 μm.

In order to non-destructively acquire precise crystallographic orientation data of lenses from Recent and fossil specimens, we used a focused ion beam (FIB) microscope to carefully remove only small portions of calcitic material (previously coated with a 20 nm layer of gold) from the top of selected lenses. FIB-based milling was usually operated at 30 kV and the following successive beam currents were typically used: 4nA; 1nA; 600 pA; 240 pA; 120 pA. Finally, low voltage (5 kV–240 pA) FIB milling was applied to remove the damaged surfaces. After this procedure, electron backscatter diffraction (EBSD) data were collected from fresh surfaces (up to about 20 x 20 μm) without coating them, using an acceleration voltage of 15–25 kV and a beam current of about 15 nA (120 μm aperture and the “high current” mode). FIB-EBSD data were acquired and processed using a Quantax CrystAlign 200 system equipped with eFlash detector installed on the Auriga 60 FIB-SEM microscope at the Faculty of Geology, University of Warsaw.

Results

Characteristic arrays of internally compact calcitic structures were identified on several isolated plates of asterozoans collected from the Wąwał locality (two radial shields and one dorsal arm plate of *Stegophiura*? and nine marginal plates of taxa belonging to the family Goniasteridae; Figs. 1d–i, 2c–g). These consist of thick imperforate stereom with a spherical top and an aspherical bottom. The fossil echinoderms have lens-like microstructures that are identical to one another and are very similar to those present in Late Cretaceous and Recent echinoderms (Gorzelak et al., 2014) (Figs. 1a–c, 2a, b). Indeed, the diameter of the structures (~40–140 μm) falls within the range of microlenses of living echinoderms (~30–150 μm) (Dubois and Hayt 1990). Detailed observations of these fossil plates using propagation-based phase-contrast synchrotron radiation X-ray tomographic microscopy confirmed that, similar to Recent light-sensitive echinoderms, internal labyrinthic stereom with trabeculae that are about 15 μm thick and irregular pores extends dorsally into a regular array of lens-like microstructures with a Huygensian shape, possibly involved in minimizing spherical aberration (Fig. 2c–e). Furthermore, the high-resolution electron backscatter diffraction data indicate that the orientation of the calcite crystallographic c-axis in these Early Cretaceous forms (Fig. 3a–d) lies parallel to the lens axis and slightly fans out at lens edges, a pattern that is also present in Recent photosensitive ophiuroids (Fig. 3e–h). This pattern was also recognized in the schizochroal lenses of trilobites and is even seen in trilobite lenses that underwent coarse recrystallization (Torney et al. 2014). This specific crystallographic orientation eliminates birefringence of calcite (division of light into two components).

Microstructural inspection of asterozoans from other localities shows that granular ornamentation on plate surfaces is not rare among older (pre-Cretaceous) ophiuroids and

asteroids. However, tubercle ornamentation patterns in Triassic–Jurassic forms are clearly different from the microlenses of Recent and Cretaceous echinoderms. First, these tubercles commonly coalesce locally to form irregular ridges and are rarely arranged in an apparently regular pattern (e.g. Villier et al. 2004; Villier 2008, Gale 2011). Furthermore, although some seem to be comprised of thin imperforate stereom, internally they are typically porous and do not exhibit a characteristic lens-like structure (Figs. 1j–l, 2h–j). Finally, in contrast to the microlenses of Recent shallow-water asterozoans, which are mainly located on the dorsal plate surface, tubercles in pre-Cretaceous forms can also occur on the ventral side (Blake et al. 2000) and may be present in deep-water taxa (Villier et al. 2009). As stressed above, the function of this granular ornamentation is not well understood; some tubercles supported moveable spines (e.g. Villier et al. 2004; Blake et al. 2000), but the function of the others is unknown.

Discussion

Echinoderms exhibit a wide range of photoreceptive abilities (e.g. Yoshida 1966; Yamamoto and Yoshida 1978; Garm and Nilsson 2014). However, in contrast to the calcitic and non-biomineralized lenses that widely occur across arthropods (e.g. Zhao et al. 2013; Torney et al. 2014), most echinoderm species appear to lack discrete organs for light perception. Photosensitivity in these echinoderms is chiefly thought to be related to diffuse dermal and/or neural light receptors, although these may be localized in specialized body parts (Delroisse et al. 2016). A key exception is the case of the calcitic microlenses possessed by some shallow-water ophiuroids (e.g. ophiocomids) and asteroids (e.g. goniasterids). Until now, however, little was known about the origins of these lens-like microstructures.

In Recent echinoderms, the external imperforate stereom layer, which is used to construct the microlenses, is formed via two phases of biomineralization, i.e. deposition of porous stereom that is secondarily filled by calcite (Heatfield 1971; Dubois and Hayt 1990). Our close examination of some dorsal arm plates of the Recent ophiuroid *O. wendtii* reveals that some microlenses are incompletely formed and are still locally porous, confirming the two-step model of their formation (Dubois and Hayt 1990) (Figs. 1a, 2a). Interestingly, tubercle ornamentation in pre-Cretaceous asterozoans examined in this study is typically internally porous, whereas it is compact and imperforate in some younger, Cretaceous forms. Based on these morphological, developmental, and paleontological data, we suggest that lens-like microstructures in Cretaceous asterozoans likely evolved by secondary deposition of calcite on the pre-existing internally porous tubercles that were already present in ancestral Jurassic forms.

It has been hypothesized that visual systems with microlenses were independently acquired in ophiuroids and asteroids by the Late Cretaceous (Gorzelak et al. 2014), and this could be linked to the onset of increased predation pressure during the Mesozoic Marine Revolution (MMR), which resulted in the evolution of many antipredatory traits in benthic organisms, including echinoderms (Vermeij 1977; Gorzelak et al. 2012; 2014). This predation hypothesis is consistent with behavioural observations of the Recent ophiuroid *O. wendtii*, which is able to escape from their predators, such as Perciformes fish, presumably thanks in part to its complex visual system (Hendler 1984). Notably, recent molecular clock analyses suggest a Late Jurassic origin of the common ancestral lineage of Perciformes fish, with a subsequent familial radiation during the Cretaceous (Wei et al. 2014). Moreover, independent data on the frequencies of sublethal arm damage (regenerating arms) in fossil ophiuroids and the temporal distributional

patterns of dense ophiuroid populations both support the hypothesis that predation pressure on ophiuroids increased in the Cretaceous (Aronson 1987, 1989, 1991).

Although a defensive function of the visual system with microlenses has yet to be tested in asteroids, it is likely that these structures might have provided an advantage not only for finding food, but also for avoiding predators, including Perciformes fish, which are likewise known to feed on asteroids (Walker 1978; Sweatman 1994).

Our new data push back the origins of this putative visual system considerably, into the Early Cretaceous. This timing is roughly coincident with the MMR, which is thought to have started during the Jurassic and continued at an accelerated pace during the Cretaceous (Vermeij 1977). The simultaneous appearance of apparently similar lens-like microstructures in two distantly-related echinoderm groups, which ancestrally lacked such traits, is a clear case of convergence. We hypothesize that some ophiuroid and asteroid lineages, occupying the same ecological niches and facing similar selective pressures, might have independently evolved similar photosensitive organs to reduce the risk of predation.

Acknowledgments

This work was completed while the first author was a recipient of a grant from the Polish National Science Centre (NCN) Grant number DEC-2011/03/N/ST10/04798 and was performed in part in the NanoFun laboratory co-financed by the European Regional Development Fund within the Innovation Economy Operational Programme POIG.02.02.00-00-025/09. IAR was funded by an 1851 Royal Commission Research Fellowship. SZ was funded by grants RYC-2012-10576 and CGL2013-48877 from the Spanish MINECO. We acknowledge the Paul Scherrer Institut, Villigen, Switzerland for the provision of synchrotron radiation beamtime on

the TOMCAT beamline at the Swiss Light Source and thank Professor Charles G Messing (Nova Southeastern University) for providing the extant ophiuroid specimen. We also thank two anonymous reviewers for their supportive comments.

Ethical standards

Investigations comply with the current laws of the country in which they were performed.

Conflict of interests

The authors declare that they have no conflict of interest.

References

- Aizenberg, J., & Hendler, G. (2004). Designing efficient microlens arrays: lessons from nature. *Journal of Materials Chemistry*, *14*, 2066–2072.
- Aizenberg, J., Tkachenko, A., Weiner, S., Addadi, L., & Hendler, G. (2001). Calcitic microlenses as part of the photoreceptor system in brittlestars. *Nature*, *412*, 819–822.
- Aronson, R.B. (1987). Predation on fossil and Recent ophiuroids. *Paleobiology*, *13*, 187–192.
- Aronson, R.B. (1989). A community-level test of the Mesozoic marine revolution theory. *Paleobiology*, *15*, 20–25.
- Aronson, R.B. (1991). Predation, physical disturbance and sub-lethal arm damage in ophiuroids: a Jurassic-Recent comparison. *Marine Ecology Progress Series*, *74*, 91–97.

248 Blake, D.B., Tintori, A., & Hagdorn, H. (2000). A new asteroid (Echinodermata) from the
 249 Norian (Triassic) Calcare di Zorzino of northern Italy: its stratigraphic occurrence and
 250 phylogenetic significance. *Rivista Italiana di Paleontologia e Stratigrafia*, 106, 141–156.

251 Cunningham, J.A., Rahman, I.A., Lautenschlager, S., Rayfield, E.J., & Donoghue, P.C.J. (2014).
 252 A virtual world of palaeontology. *Trends in Ecology & Evolution*, 29, 347–357.

253 Delroisse, J., Mallefet, J. & Flammang, P. (2016). De Novo Adult Transcriptomes of Two
 254 European Brittle Stars: Spotlight on Opsin-Based Photoreception. *PLoS ONE*,
 255 11:e0152988. doi:10.1371/journal.pone.0152988

256 Döderlein, L. (1898). Ueber "Krystallkörper" bei Seesternen. *Denkschriften der Medizinisch*
 257 *Naturwissenschaftlichen Gesellschaft zu Jena*, 8, 491-494.

258 Dubois, P., & Hayt, S. (1990). Ultrastructure des ossicules d'échinodermes à stéréome non
 259 perforé. In C., De Ridder, P., Dubois, M.C., Lahaye, & M., Jangoux (Eds.), *Echinoderm*
 260 *Research*: (pp. 217–223). Rotterdam, Balkema.

261 Gale, A. (2011). Asteroidea (Echinodermata) from the Oxfordian (Late Jurassic) of Savigna,
 262 Département [sic!] du Jura, France. *Swiss Journal of Palaeontology*, 130, 69–89.

263 Garm, A., & Nilsson, D.E. (2014). Visual navigation in starfish: first evidence for the use of
 264 vision and eyes in starfish. *Proceedings of the Royal Society B: Biological Sciences*, 281,
 265 2013–3011.

266 Gorzelak, P., & Salamon, M.A. (2009). Signs of benthic predation on Late Jurassic stalked
 267 crinoids, preliminary data. *Palaios*, 24, 70–73.

268 Gorzelak, P., Salamon, M.A., & Baumiller, T.K. (2012). Predator-induced macroevolutionary
 269 trends in Mesozoic crinoids. *Proceedings of the National Academy of Sciences of the*
 270 *United States of America*, 109, 7004–7007.

271 Gorzelak, P., Salamon, M.A., Lach, R., Loba, M., & Ferré, B. (2014). Microlens arrays in the
 272 complex visual system of Cretaceous echinoderms. *Nature Communications*, 5:3576, doi:
 273 10.1038/ncomms4576.

274 Heatfield, B.M. (1971). Growth of the calcareous skeleton during regeneration of spines of the
 275 sea urchin *Strongylocentrotus purpuratus* (Stimpson); a light and scanning electron
 276 microscope study. *Journal of Morphology*, 134, 57–90.

277 Hendler, G. (1984). Brittlestar color-change and phototaxis (Echinodermata: Ophiuroidea:
 278 Ophiocomidae). *Marine Ecology*, 5, 379–401.

279 Hendler, G., & Byrne, M. (1987). Fine structure of the dorsal arm plate of *Ophiocoma wendti*
 280 (Echinodermata, Ophiuroidea). *Zoomorphology*, 107, 261–272.

281 Hendler, G. (2004). An echinoderm's eye view of photoreception and vision. In T. Heinzeller, &
 282 J. Nebelsick (Eds.), *Echinoderms; Munchen; Proceedings of the 11th International*
 283 *Echinoderm Conference*. (pp. 339-350). Leiden: A.A. Balkema Publishers.

284 Hess, H., Salamon, M.A., & Gorzelak, P. (2011). Late Jurassic-Early Cretaceous (Tithonian-
 285 Berriasian) cyrtocrinids from south-eastern Poland. *Neues Jahrbuch für Geologie und*
 286 *Paläontologie, Abhandlungen*, 260, 119–128.

287 Kaim, A. (2001). Faunal dynamics of juvenile gastropods and associated organisms across the
 288 Valanginian transgression-regression cycle in central Poland. *Cretaceous Research*, 22,
 289 333-351.

290 Killian, C.E., & Wilt, F.H. (2008). Molecular aspects of biomineralization of the echinoderm
 291 endoskeleton. *Chemical Reviews*, 108, 4463–4474.

292 Mah, C.L. (2005). A phylogeny of *Iconaster* and *Glyphodiscus* (Goniasteridae; Valvatida;
 293 Asteroidea) with descriptions of four new species. *Zoosystema*, 27, 131–167.

294 Politi, Y., Arad, T., Klein, E., Weiner, S., & Addadi, L. (2004). Sea urchin spine calcite forms
 295 via a transient amorphous calcium phase. *Science*, 306, 1161–1164.

296 Raup, D.M. (1966). The endoskeleton. In R.A. Boolootian (Ed.), *Physiology of Echinodermata*
 297 (pp. 379–395). New York: Interscience.

298 Salamon, M.A. (2008). The Callovian (Middle Jurassic) crinoids from northern Lithuania.
 299 *Paläontologische Zeitschrift*, 82, 269–278.

300 Salamon, M.A. (2009). Early Cretaceous (Valanginian) sea lilies (Echinodermata, Crinoidea)
 301 from Poland. *Swiss Journal of Geosciences*, 102, 77–88.

302 Salamon, M.A., & Zatoń, M. (2007). Late Bajocian through Callovian (Middle Jurassic) crinoid
 303 fauna from the epicontinental deposits of Poland. *Swiss Journal of Geosciences*, 100, 153–
 304 164.

305 Salamon, M.A., & Gorzelak, P. (2010). Cyrtocrinids (Echinodermata, Crinoidea) from Upper
 306 Jurassic Štramberk-type limestones in southern Poland. *Palaeontology*, 53, 869–885.

307 Salamon, M.A., Niedźwiedzki, R., Lach, R., Brachaniec, T., & Gorzelak, P. (2012). Ophiuroids
 308 Discovered in the Middle Triassic Hypersaline Environment. *PLoS ONE*, 7(11): e49798.
 309 doi:10.1371/journal.pone.0049798.

310 Smith, A.B. (1990). Biomineralization in echinoderms. In J.G. Carter (Ed.), *Skeletal*
 311 *biomineralization: patterns, processes, and evolutionary trends* (pp. 413–443). New York:
 312 Van Nostrand Reinhold.

313 Stampanoni, M., et al. (2007). TOMCAT: a beamline for tomographic microscopy and coherent
 314 radiology experiments. *AIP Conference Proceedings*, 879, 848.

315 Sutton, M.D., Rahman, I.A., & Garwood, R.J. (2014). *Techniques for Virtual Palaeontology*.
 316 Wiley.

317 Sweatman, H.P.A. (1995). A field study of fish predation on juvenile crown-of-thorns starfish.
318 Coral reefs, *14*(1), 47-53.

319 Torney, C., Lee, M.R., & Owen, A.W. (2014). Microstructure and growth of the lenses of
320 schizochroal trilobite eyes. *Palaeontology*, *57*, 783–799.

321 Ullrich-Lüter, E.M, Dupont, S., Arboleda, E., Hausen, H., & Arnone, M.I. (2011). Unique
322 system of photoreceptors in sea urchin tube feet. *Proceedings of the National Academy of*
323 *Sciences of the United States of America*, *108*, 8367–8372.

324 Vermeij, G.J. (1977). The Mesozoic marine revolution; evidence from snails, predators and
325 grazers. *Paleobiology*, *3*, 245–258.

326 Villier, L. (2008). Sea star ossicles from the Callovian black clays of the Łuków area, eastern
327 Poland. *Neues Jahrbuch für Geologie und Paläontologie, Abh.*, *247*, 147–160.

328 Villier, L., Charbonnier, S., & Riou, B. (2009). Sea stars from Middle Jurassic Lagerstätte of La
329 Volute sur Rhône (Ardèche, France). *Journal of Paleontology*, *83*, 389–398.

330 Villier, L., Kutscher, M., & Mah, C.H.L. (2004). Systematics and palaeology of middle
331 Toarcian Asteroidea (Echinodermata) from the ‘Seuil du Poitou’, Western France.
332 *Geobios*, *37*, 807–825.

333 Vinogradova, E., Ruíz-Zepeda, F., Plascencia-Villa, G., & José-Yacamán, M. (2016). Calcitic
334 microlens arrays in *Archaster typicus*: microstructural evidence for an advanced
335 photoreception system in modern starfish. *Zoomorphology*, *135*, 83–87.

336 Walker, M.H. (1978). Food and feeding habits of *Lethrinus chrysostomus* Richardson (Pisces:
337 Perciformes) and other Lethrinids on the Great Barrier Reef. *Australian Journal of Marine*
338 *& Freshwater Research* *29*(5):623-30.

- Wei, T., Sun, Y., Zhang, B., Wang, R., & Xu, T. (2014). A Mitogenomic Perspective on the Phylogenetic Position of the *Haploidenys* Genus (Acanthopterygii: Perciformes) and the Evolutionary Origin of Perciformes. *PLoS ONE*, 9(7), e103011. doi:10.1371/journal.pone.0103011
- Yamamoto, M., & Yoshida, M. (1978). Fine structure of the ocelli of a synaptid holothurian, *Opheodesoma spectabilis*, and the effects of light and darkness. *Zoomorphologie*, 90, 1–17.
- Yoshida, M. (1966). Photosensitivity. In R.A. Boolootian (Ed.), *Physiology of Echinodermata* (pp. 435–464). New York: John Wiley & Sons.
- Zaton, M., Salamon, M.A., Boczarowski, A., & Sitek, S. (2008). Taphonomy of dense ophiuroid accumulations from the Middle Triassic of Poland. *Lethaia*, 41(1), 47–58.
- Zhang, S. (2003). Fabrication of novel biomaterials through molecular self-assembly. *Nature Biotechnology*, 21, 1171–1178.
- Zhao, F., Bottjer, D.J., Hu, S., Yin, Z., & Zhu, M. (2013). Complexity and diversity of eyes in Early Cambrian ecosystems. *Scientific Reports*, 3, 2751, doi:10.1038/srep02751

FIGURE CAPTIONS

Fig. 1. Skeletal microstructure of extant and fossil asterozoans. The images are scanning electron micrographs (SEM). **(a–c)** Microlenses on a dorsal arm plate (DAP) of the Recent ophiuroid *Ophiocoma wendtii* (ZPALV.42REC_op1); arrows in **(a)** show incompletely formed microlenses. **(b)** Magnification of a single lens. **(c)** Cross-section of a fractured single lens. **(d–f)** Microlenses on a radial shield of the Early Cretaceous (Valanginian) ophiuroid *Stegophiura?*

(GIUS 9-3468o1). **(e)** Magnification of a single lens. **(f)** Cross-section of a fractured single lens. **(g-i)** Microlenses on a marginal plate of an Early Cretaceous (Valanginian) asteroid belonging to the family Goniasteridae (GIUS 9-3468a1). **(h)** Magnification of a single lens. **(i)** Cross-section of a fractured single lens. **(j-l)** Granular ornamentation on a marginal plate of a Late Jurassic asteroid belonging to the family Goniasteridae (GIUS 8-3577a1). **(k)** Magnification of a single tubercle. **(l)** Cross-section of a fractured single tubercle. Dotted lines indicate lens morphology.

Fig. 2. Synchrotron slices illustrating internal microstructure of extant and fossil echinoderms.

(a, b) Contact (delineated by dotted line in **(b)**) between microlenses (L) comprised of compact imperforate stereom layer and the underlying porous labyrinthic stereom (S) in a dorsal arm plate (DAP) of the Recent ophiuroid *Ophiocoma wendtii* (ZPALV.42REC_op1); slices aligned perpendicularly **(a)** or longitudinally **(b)** to the ossicle surface, arrows show incompletely formed microlenses. **(c-e)** Contact (delineated by dotted lines) between microlenses (L) forming a compact imperforate stereom layer and the underlying porous labyrinthic stereom (S) in a marginal plate of an Early Cretaceous (Valanginian) asteroid belonging to the family Goniasteridae (GIUS 9-3468a1); slices aligned perpendicularly to the ossicle surface. **(f, g)** Examples (arrows) of characteristic “spoke-like” appearance of lens-like microstructure in a marginal plate of an Early Cretaceous (Valanginian) asteroid belonging to the family Goniasteridae (GIUS 9-3468a1) **(f)** and the ophiuroid *Stegophiura?* (GIUS 9-3468o1) **(g)** slices aligned longitudinally to the ossicle surface close to the dorsal side. **(h-j)** Coarse rectilinear or labyrinthic stereom (S) homogenously distributed within the marginal plates with granular ornamentation of a Late Jurassic asteroid belonging to the family Goniasteridae (GIUS 8-3577a1); slices aligned perpendicularly **(h)** or longitudinally **(i, j)** to the ossicle surface.

385

386 **Fig. 3.** Crystallographic data obtained from fossil and Recent echinoderms. **(a)** SEM micrograph
387 of the lens of the Valanginian ophiuroid *Stegophiura?* (GIUS 9-3468o1) after FIB treatment
388 showing lens and calcite c-axis (red dotted line); dotted black rectangle indicates region
389 sectioned almost perpendicular to the lens axis from which EBSD data were collected **(b-d)**. **(b)**
390 Pole figure with the orientation of the calcite c-axis in **(d)**. **(c)** Graph showing misorientation
391 across the white line shown in **(d)**, implying the presence of subdomains. **(d)** Combined
392 diffraction intensity and crystallographic orientation data with key to colour coding; the uniform
393 colour of calcite implies a uniform crystallographic orientation, dark areas in the interior indicate
394 poor diffraction due to the irregular topography after FIB treatment. **(e)** SEM micrograph of the
395 lens of the Recent ophiuroid *Ophiocoma wendtii* (ZPALV.42REC_op1) after FIB treatment
396 showing lens and calcite c-axis (red dotted line); dotted black rectangle indicates region
397 sectioned almost perpendicular to the lens axis from which EBSD data were collected **(f-h)**. **(f)**
398 Pole figure showing the orientation of the calcite c-axis in **(h)**. **(g)** Graph showing misorientation
399 across the white line shown in **(h)**, implying the presence of subdomains. **(h)** Combined
400 diffraction intensity and crystallographic orientation data with key to colour coding; the uniform
401 colour of calcite implies a uniform crystallographic orientation, dark areas in the interior indicate
402 poor diffraction due to irregular topography after FIB treatment and/or presence of organic
403 inclusions.

404

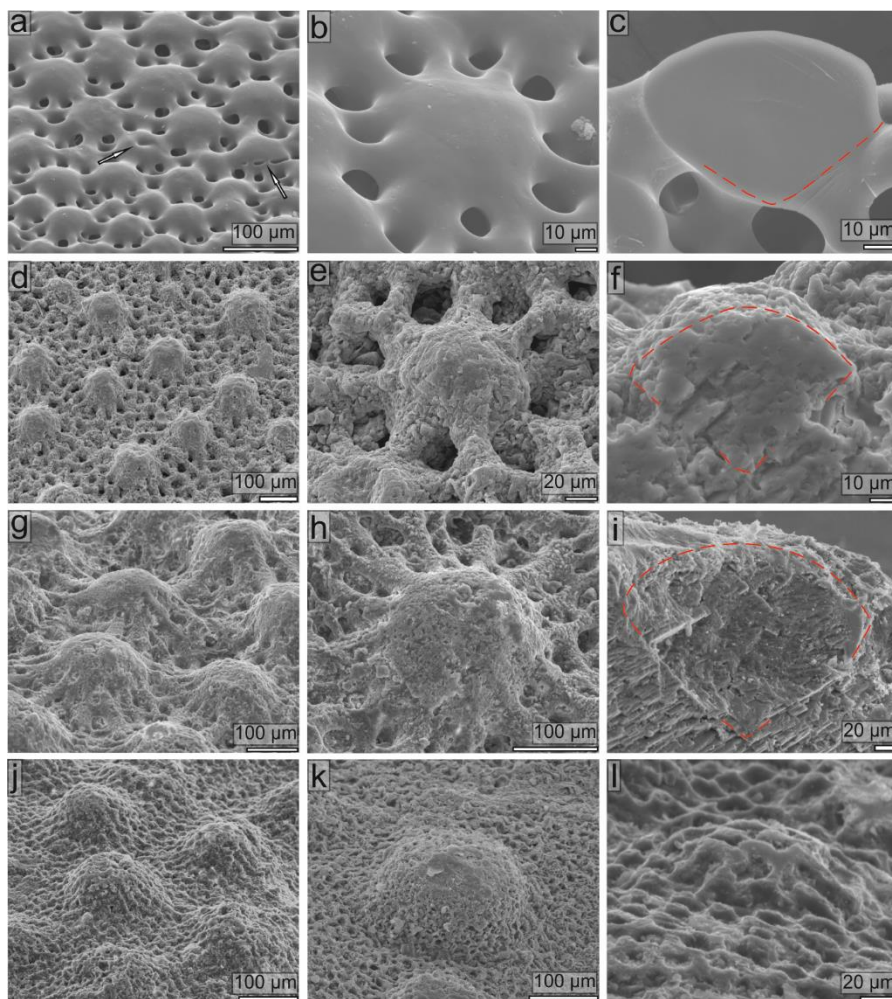


Fig. 1.

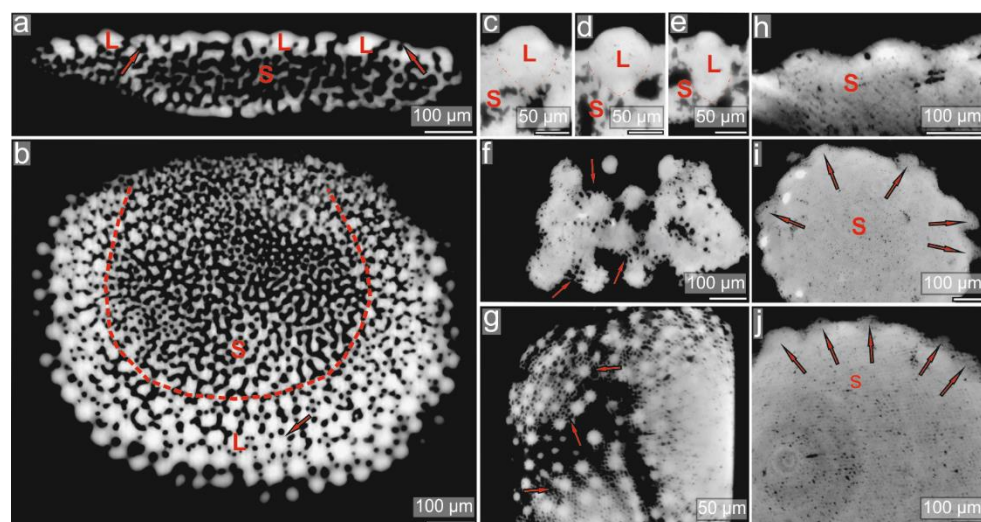


Fig. 2.

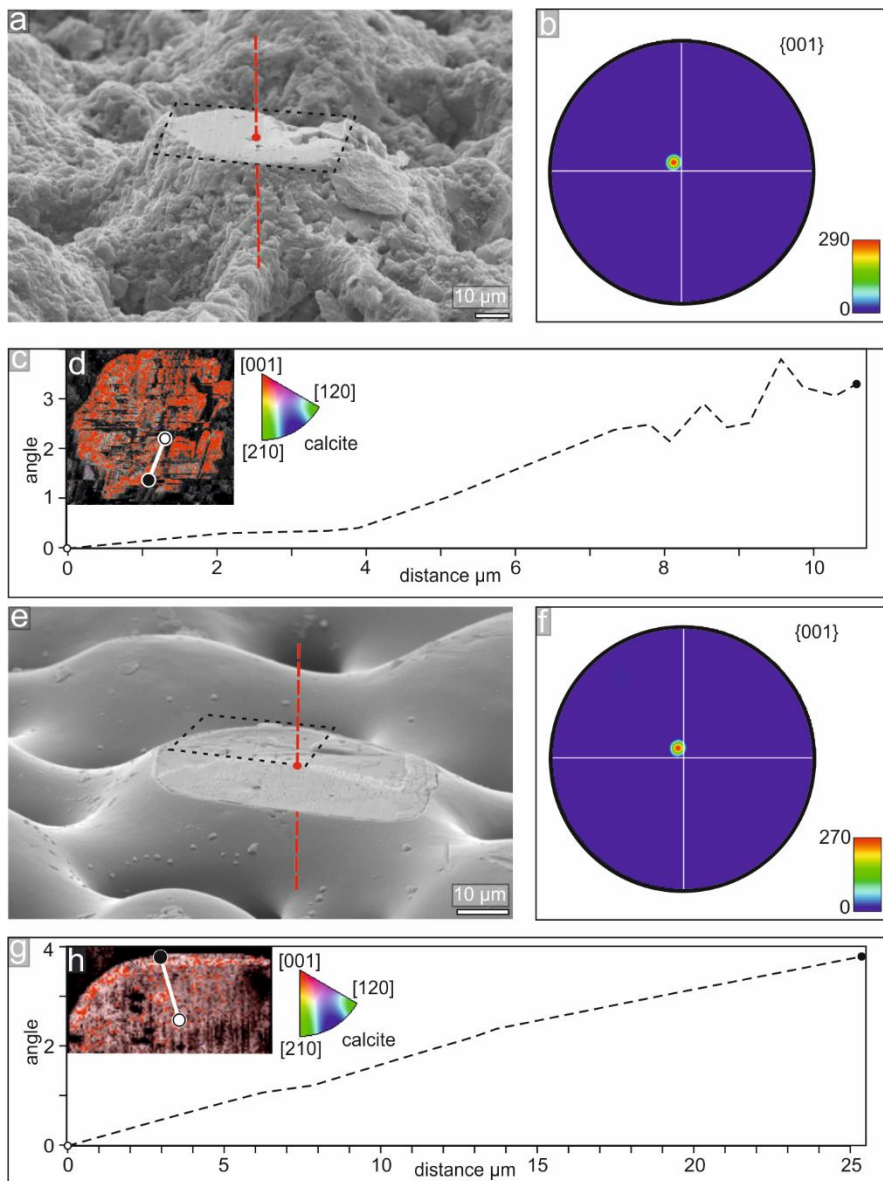


Fig. 3.